# Jets at Hadron Colliders

Nigel Glover (IP3, Durham)

June 2001

- Introduction and Kinematics
- $2 \rightarrow 2$ scattering
  - phase space
  - parton level cross section
  - matrix elements
  - single effective subprocess
  - parton-parton luminosity
  - scaling violations
  - unphysical scales
- NLO
  - why?
  - phase space
  - matrix elements and limits
  - scale dependence
  - jet algorithms
  - jet shapes

# Typical hard scattering event

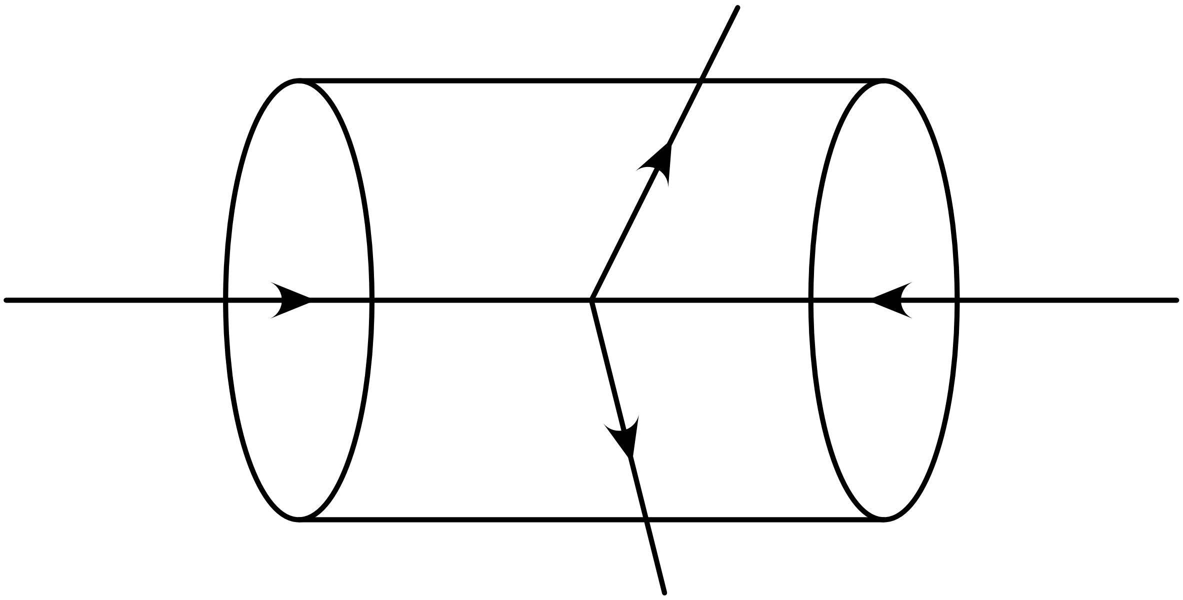

Two clear jets, separated in azimuth by $\pi$ radians

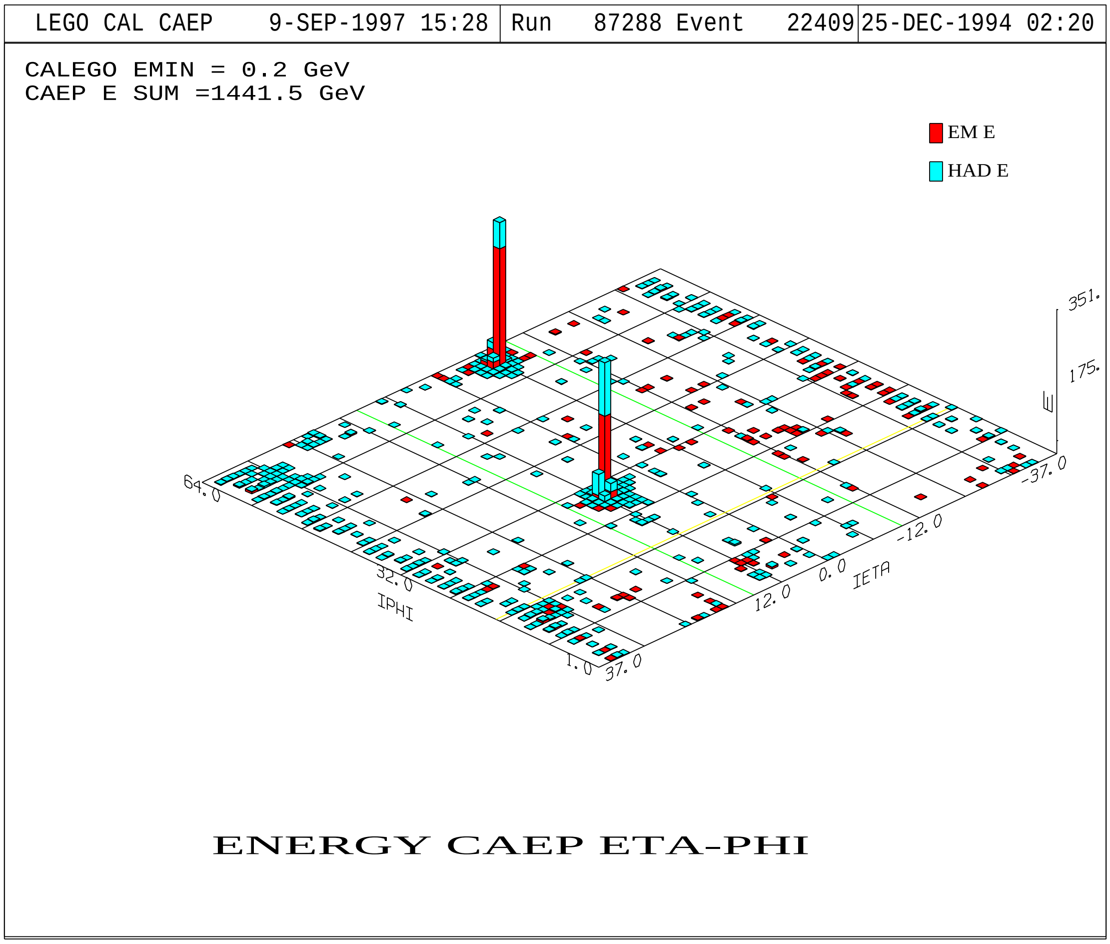

# The side view

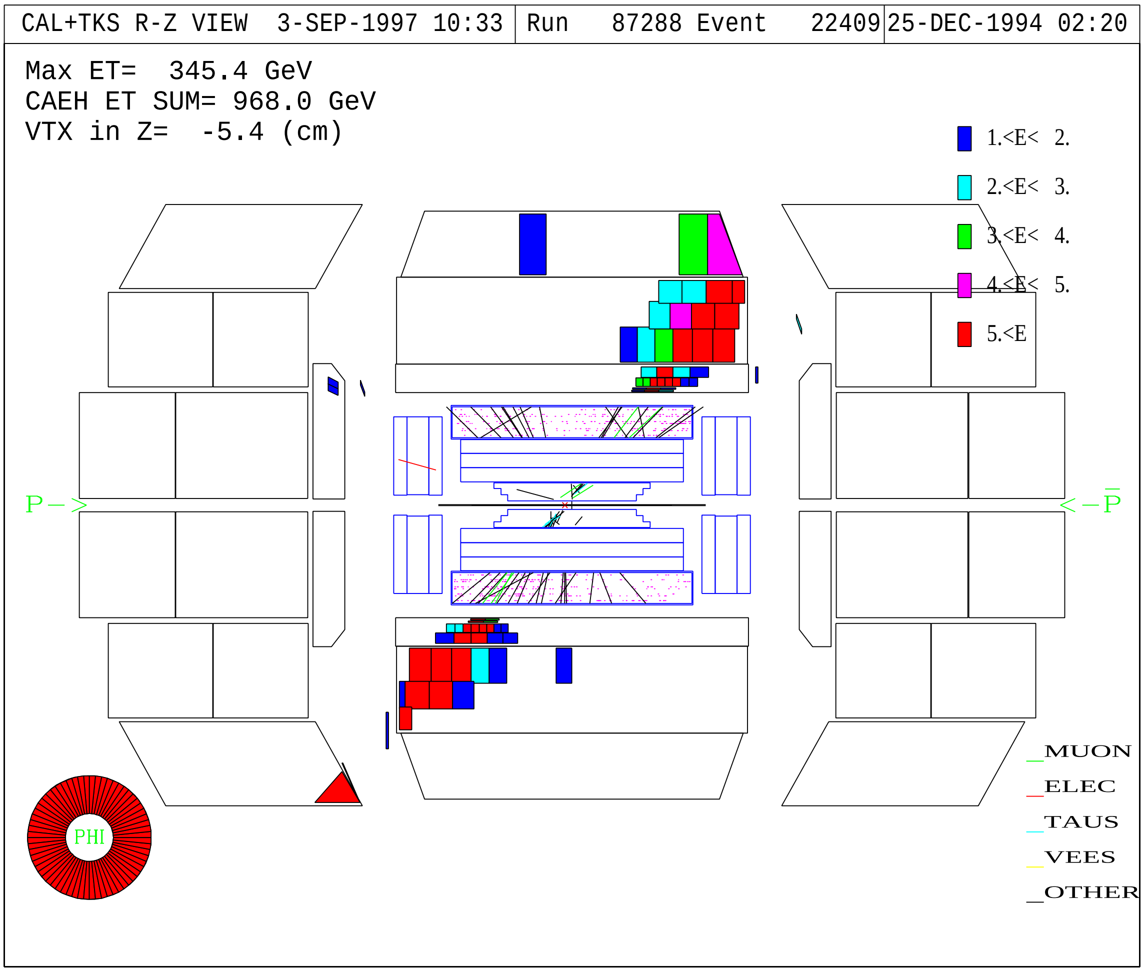

# Kinematics in Hadronic Collisions

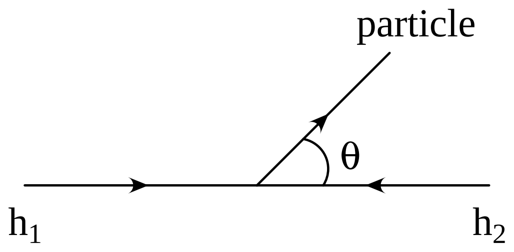


- Rapidity ($y$)

$$y \equiv \frac{1}{2}\ln\left(\frac{E+p_z}{E-p_z}\right) = \frac{1}{2}\ln\left(\frac{1+\beta\cos\theta}{1-\beta\cos\theta}\right)$$

- Pseudo-rapidity $\eta$

  In the high energy limit, $\beta \longrightarrow 1$ or $m \longrightarrow 0$ then,

$$\eta \equiv \frac{1}{2}\ln\left(\frac{1+\cos\theta}{1-\cos\theta}\right) = -\ln\left(\tan\left(\theta/2\right)\right)$$

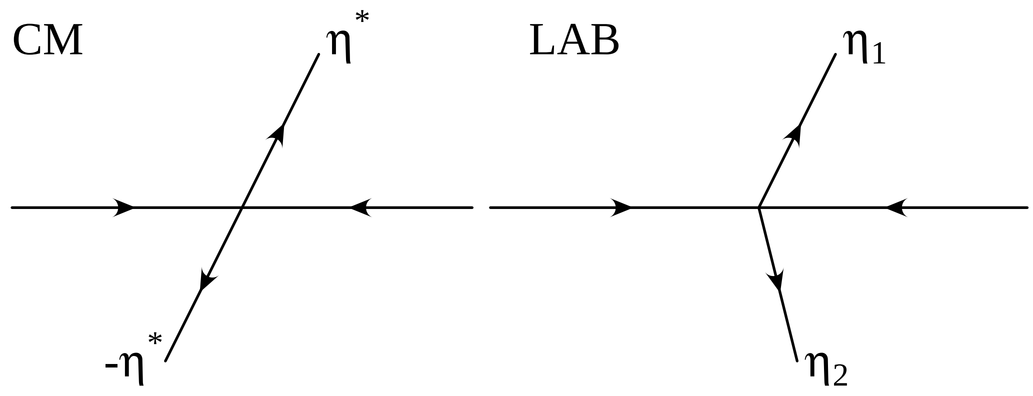


$$\eta^* = \frac{1}{2}(\eta_1 - \eta_2), \;\; \eta^{\mathrm{boost}} = \frac{1}{2}(\eta_1 + \eta_2)$$

$$\eta_{\mathrm{LAB}} = \eta^* + \eta^{\mathrm{boost}}$$

# Kinematics in Hadronic Collisions cont'd

- Transverse energy $E_T$

$$E_T^2 = m^2 + p_x^2 + p_y^2 = m^2 + p_T^2 = E^2 - p_z^2$$

$$\begin{aligned} p_T &= p \sin\theta \\ p_z &= E \tanh y = E_T \sinh y \\ E &= E_T \cosh y \end{aligned}$$

For massless particles,

$$E_T \to p_T$$

- Invariant Mass

$$M_{12}^2 = (p_1 + p_2)^2 = m_1^2 + m_2^2 + 2(E_1 E_2 - \vec{p_1} \cdot \vec{p_2})$$

For massless particles,

$$M_{12}^2 \to 2E_{T1}E_{T2}(\cosh\Delta\eta - \cos\Delta\phi)$$

# Kinematics for $2 \to 2$ scattering

To orient ourselves in the $\eta_1 - \eta_2$ plane, we first focus on the allowed phase space in terms of $\eta_1$ and $\eta_2$. At lowest order, the jet pseudorapidities are directly related to the parton fractions by

$$\begin{aligned} x_1 &= \frac{E_T}{\sqrt{s}} \left( \exp(\eta_1) + \exp(\eta_2) \right), \\ x_2 &= \frac{E_T}{\sqrt{s}} \left( \exp(-\eta_1) + \exp(-\eta_2) \right). \end{aligned}$$

Since the momentum fraction cannot exceed unity, we find,

$$-\log\left(\frac{2 - x_T \exp(-\eta_1)}{x_T}\right) < \eta_2 < \log\left(\frac{2 - x_T \exp(\eta_1)}{x_T}\right),$$

and,

$$|\eta_1| < \cosh^{-1}\left(\frac{1}{x_T}\right),$$

where $x_T = 2E_T/\sqrt{s}$ and $x_T^2 < x_1 x_2 < 1$.

Exercise: prove these boundaries on $\eta_1$ and $\eta_2$

# Phase space for $2 \to 2$ scattering

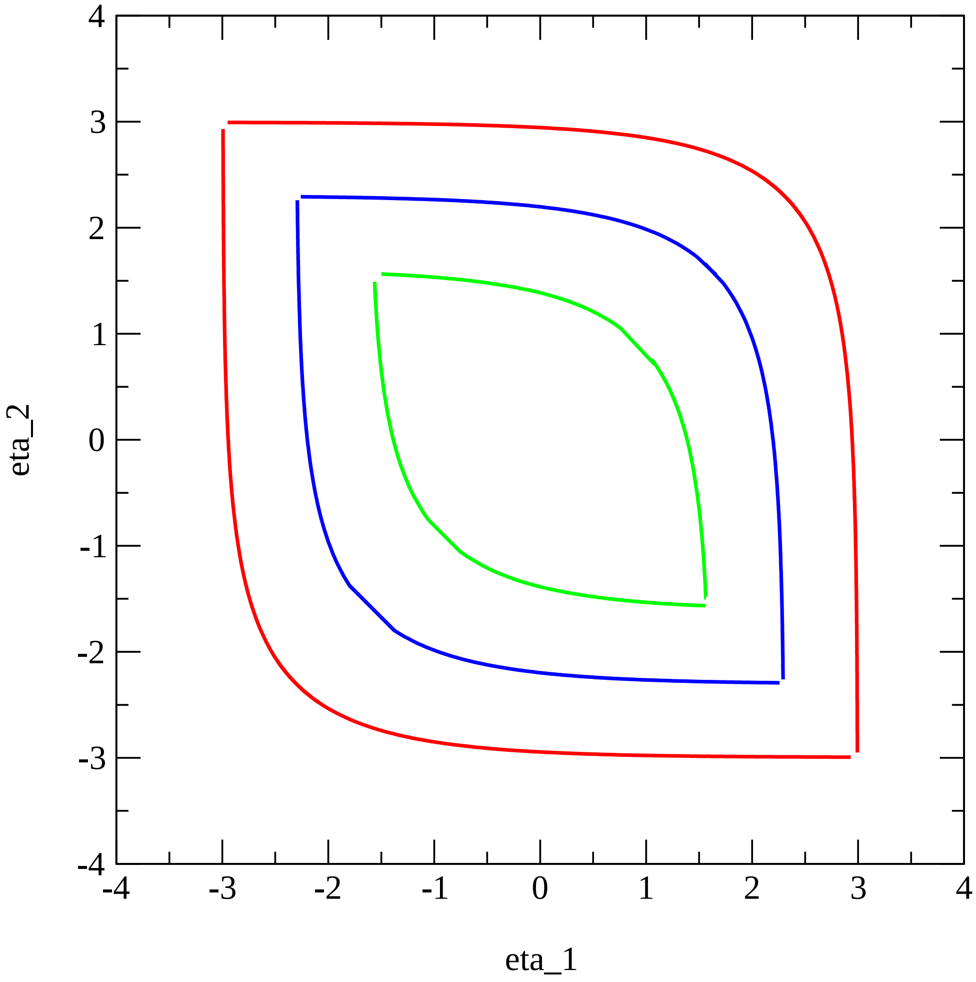


Figure 1: Phase space boundary for jets of $E_T = 100$, $200$ and $400$ GeV at $\sqrt{s} = 2$ TeV.

- As $E_T$ increases, the allowed phase space shrinks.
- for $\eta_1 \sim -\eta_2$, the energy of the particles approaches the beam energy
- for $\eta_1 \sim +\eta_2$, $M_{12}^2 \sim 4E_T^2$

# Phase space for $2 \rightarrow 2$ scattering

Kinematics determined by $E_T$, $\eta_1$ and $\eta_2$.

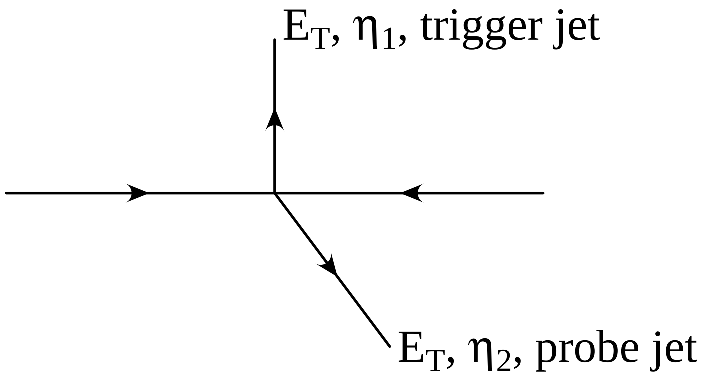


$\Longrightarrow$ observe triple differential cross section $d^3\sigma/dE_T d\eta_1 d\eta_2$

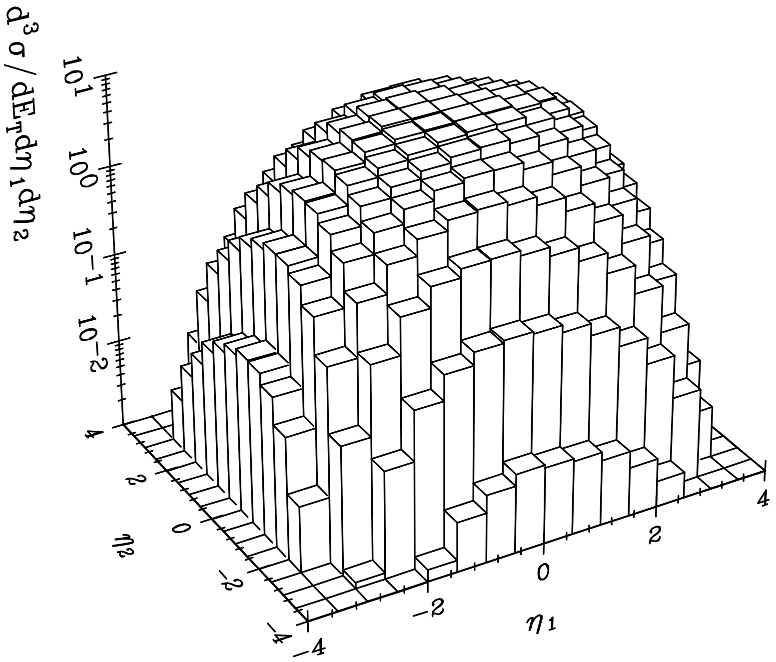


Many different observables;

- Single jet inclusive $E_T$ distribution
- Same-side to Opposite-side jet ratio

# Phase space for $2 \to 2$ scattering cont'd

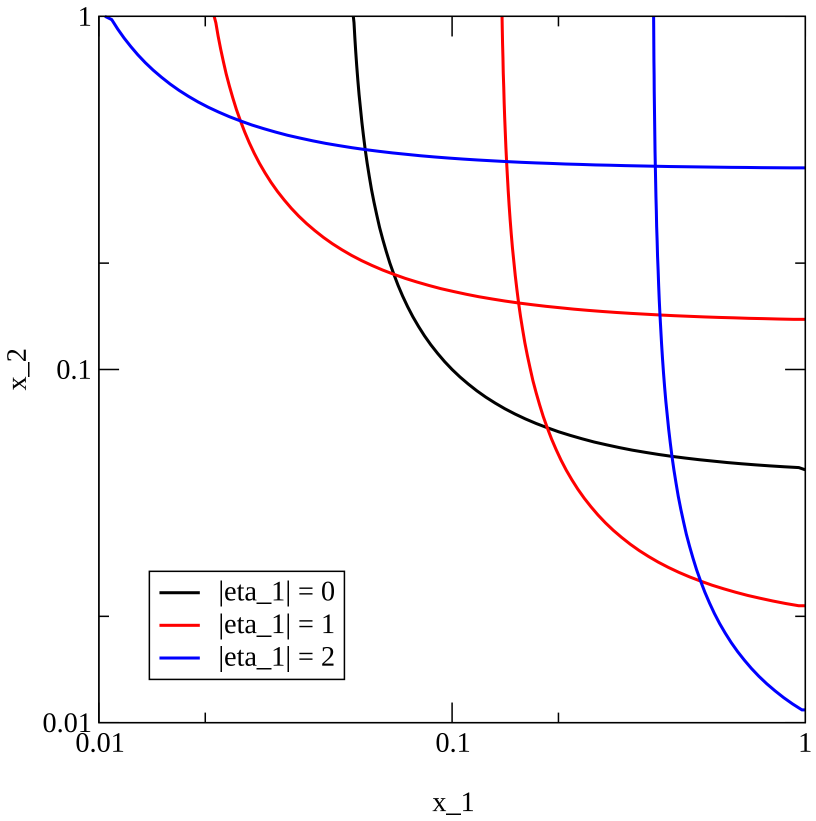


Figure 2: Phase space boundary for jets of $E_T = 100$ GeV and $|\eta_1| = 0$, $|\eta_1| = 1$ and $|\eta_1| = 2$ at $\sqrt{s} = 2$ TeV.

# Cross section for jet production

In terms of the natural kinematic variables, the cross section for two jet production at leading order is given by

$$\frac{d^3\sigma}{dE_T d\eta_1 d\eta_2} = \frac{1}{8\pi}\sum_{ij} x_1 f_i(x_1,\mu_F)\; x_2 f_j(x_2,\mu_F) \times \frac{\alpha_s^2(\mu_R)}{E_T^3}\frac{|\mathcal{M}_{ij}(\eta^*)|^2}{\cosh^4\eta^*},$$

where

- $f_i(x,\mu_F)$ $(i=g,q,\bar{q})$ represents the density of parton $i$ in the proton at factorisation scale $\mu_F$
- $|\mathcal{M}_{ij}|^2$ is the lowest order squared matrix element for $ij \to 2$ partons summed and averaged over initial and final state spins and colours.
- For parton-parton scattering, many subprocesses contribute; $qq \to qq$, $q\bar{q} \to q\bar{q}$, $qg \to qg$, $gg \to gg$, etc etc;

# Spin averaged lowest order matrix elements

The matrix elements for

$$a(p_1) + b(p_2) \to c(p_3) + d(p_4)$$

averaged (summed) over initial (final) state colours and spins

| Process | $\sum \lvert M\rvert^2/g^4$ |
|---|---|
| $q\bar{q} \to q'\bar{q}'$ | $\frac{4}{9}\frac{u^2+t^2}{s^2}$ |
| $q\bar{q} \to q\bar{q}$ | $\frac{4}{9}\left(\frac{u^2+t^2}{s^2} + \frac{u^2+s^2}{t^2}\right) - \frac{8}{27}\frac{u^2}{st}$ |
| $qg \to qg$ | $\frac{u^2+s^2}{t^2} - \frac{4}{9}\frac{u^2+s^2}{su}$ |
| $gg \to gg$ | $\frac{9}{2}\left(3 - \frac{ut}{s^2} - \frac{us}{t^2} - \frac{ts}{u^2}\right)$ |

where $s = (p_1 + p_2)^2$, $t = (p_1 - p_3)^2$ and $u = (p_2 - p_3)^2$ are the Mandelstam variables.

The matrix elements for other processes are obtained by crossing - e.g.

$$\sum |M|^2_{q\bar{q}' \to q\bar{q}'}(s,t,u) = \sum |M|^2_{q\bar{q} \to q'\bar{q}'}(t,s,u)$$

since we make the exchange $q \leftrightarrow q'$, $p_2 \leftrightarrow -p_3$ or $s \leftrightarrow t$.

Exercise: find expressions for $\sum |M|^2_{q\bar{q} \to gg}$ and $\sum |M|^2_{gg \to q\bar{q}}$

# Spin averaged lowest order matrix elements contd

In fact, all of the various matrix elements have very similar shap

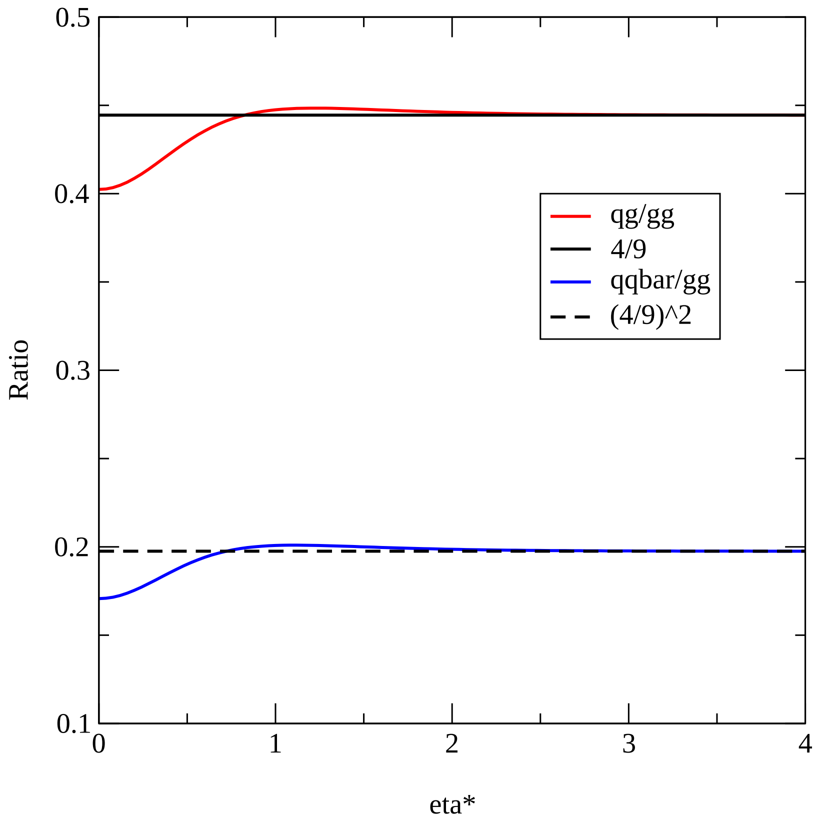


Figure 3: Ratios of matrix elements for $qg/gg$ and $q\bar{q}/gg$ as a function of the centre-of-mass rapidity $\eta^*$

we see that

$$\sum |M|^2_{gq\to gq} + \sum |M|^2_{gq\to qg} \sim \frac{4}{9} \sum |M|^2_{gg\to gg}$$

and similarly for quark initiated processes

$\Longrightarrow$ The single effective subprocess

# The single effective subprocess

Can write the lowest order cross section approximately as

$$\frac{d^3\sigma}{dE_T d\eta_1 d\eta_2} \sim \frac{1}{8\pi}\, x_1 F(x_1,\mu_F)\; x_2 F(x_2,\mu_F) \times \frac{\alpha_s^2(\mu_R)}{E_T^3}\frac{|\mathcal{M}_{gg\to gg}|^2}{\cosh^4\eta^*},$$

where $F(x,\mu)$ is the single effective parton density,

$$F(x,\mu) = g(x,\mu) + \frac{4}{9}\sum_q \left(q(x,\mu)+\bar{q}(x,\mu)\right).$$

The sum over parton subprocesses is accounted for by $F(x,\mu)$.

$\Longrightarrow$ Can understand jet cross sections at lowest order in terms of

- Gluonic matrix elements
- $F(x,\mu)$

# Gluonic matrix elements

The parton-parton subprocess scattering matrix elements are independent of $\eta^{\text{boost}}$ so the only variation is with the centre-of-mass rapidity $\eta^*$,

$$\frac{|\mathcal{M}_{gg\to gg}|^2}{\cosh^4(\eta^*)} = \frac{9\pi^2}{8}\frac{(4\cosh^2(\eta^*)-1)^3}{\cosh^6(\eta^*)}.$$

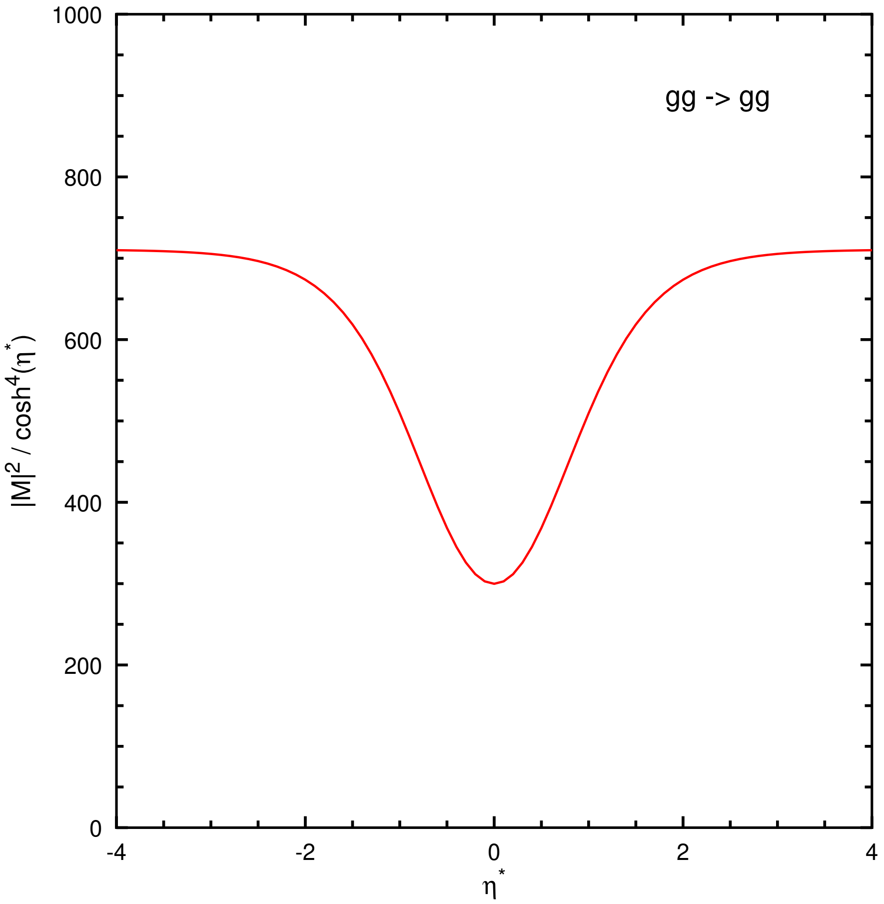


As $|\eta^*|$ gets large, $t$ (or $u$) $\to 0$ and we approach the regge limit.

# Parton luminosity

The parton-parton luminosity in the single effective subprocess approximation as a function of $\eta^{\rm boost}$ for different $|\eta^*|$ values ($E_T = 100$ GeV and $\sqrt{s} = 2$TeV). This corresponds to diagonal strips across the $\eta_1 - \eta_2$ plane.

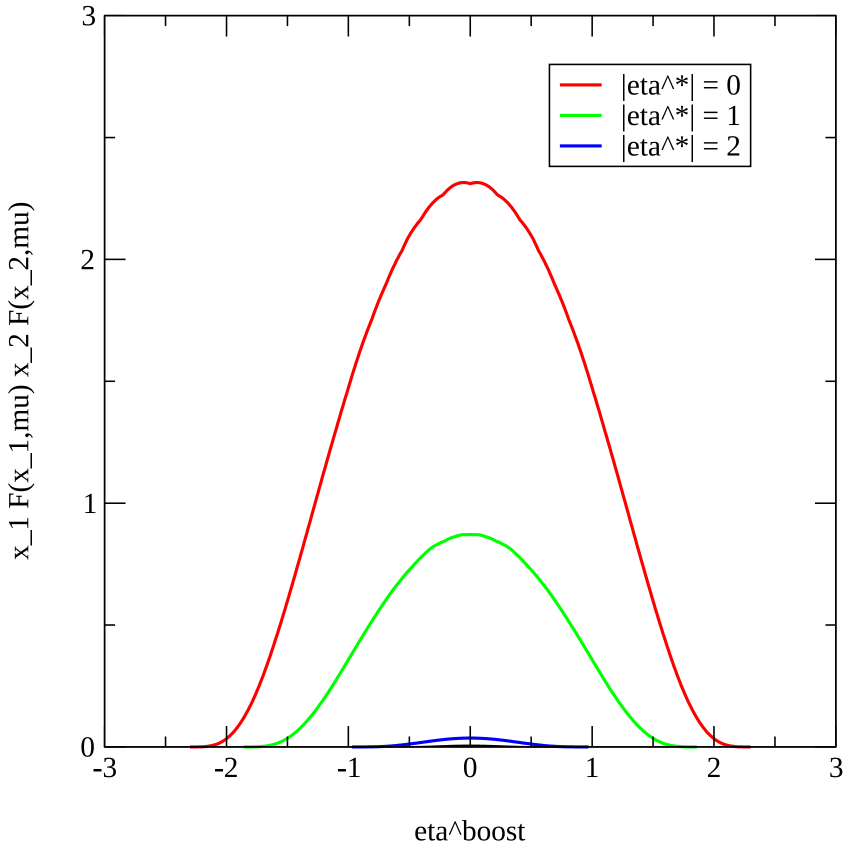


As expected, the largest luminosity occurs when $x_1$ and $x_2$ are equally small, $\eta^* \sim \eta^{\rm boost} = 0$. As either $|\eta^{\rm boost}|$ or $|\eta^*|$ increases, the luminosity decreases rapidly. However the falloff is more rapid with increasing $|\eta^*|$ than with increasing $|\eta^{\rm boost}|$.

# Gluon v Quark contribution

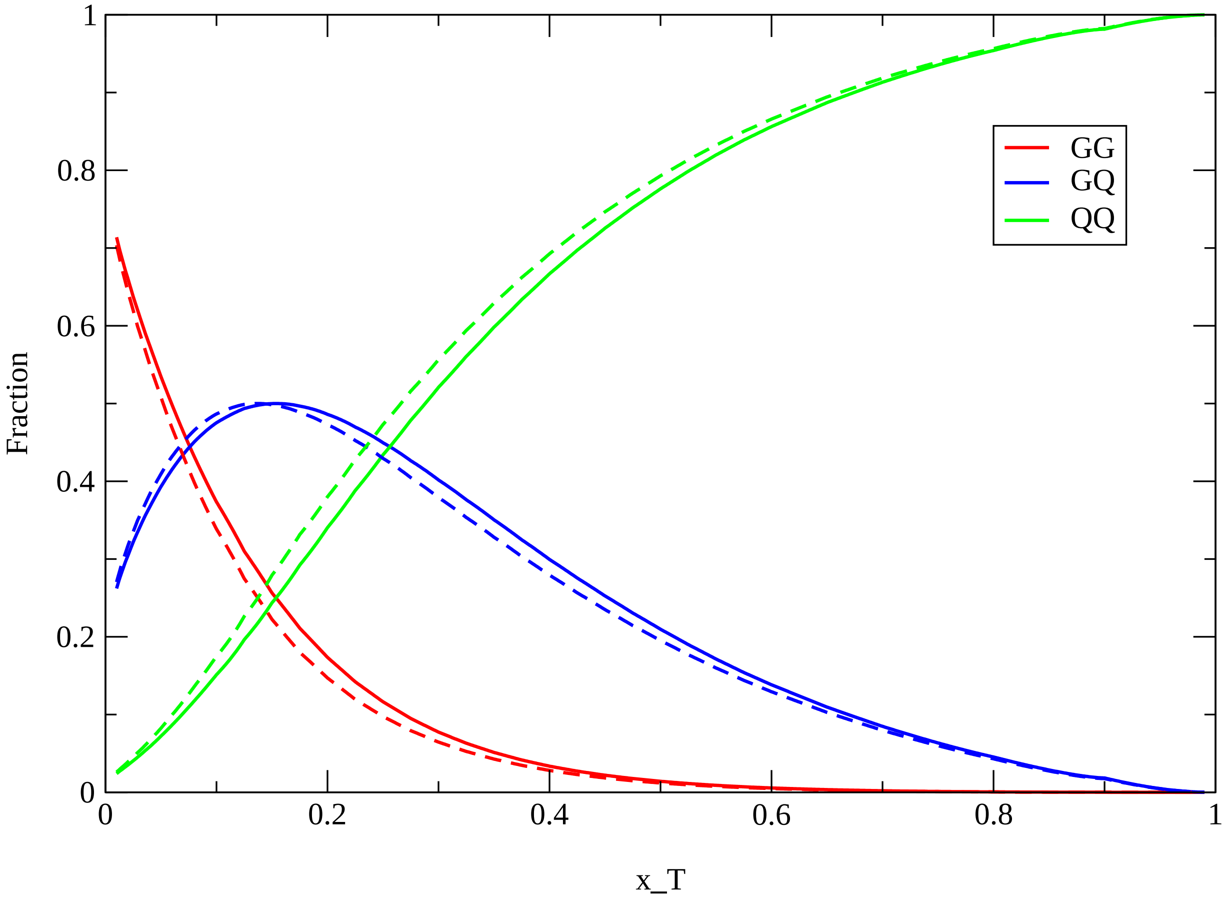


Figure 4: Fraction of cross section from gluon-gluon, gluon-quark and quark-quark processes at $\eta_1 = \eta_2 = 0$ at $\sqrt{s} = 2$ TeV (solid) and $\sqrt{s} = 14$ TeV (dashed) $x_T = 2E_T/\sqrt{s}$.

Mostly gluon initial state at low $x_T$ and quark initiated at large $x_T$.

At $x_T \sim 0.5$, gluons responsible for 20% of cross section.

# Scaling cross section

The scaled cross section is independent of $\sqrt{s}$

$$E_T^3 \frac{d^3\sigma}{dE_T d\eta_1 d\eta_2} \sim \frac{1}{8\pi} \, x_1 F(x_1, \mu_F) \; x_2 F(x_2, \mu_F)$$
$$\times \quad \alpha_s^2(\mu_R) \frac{|\mathcal{M}_{gg\to gg}|^2}{\cosh^4 \eta^*}$$

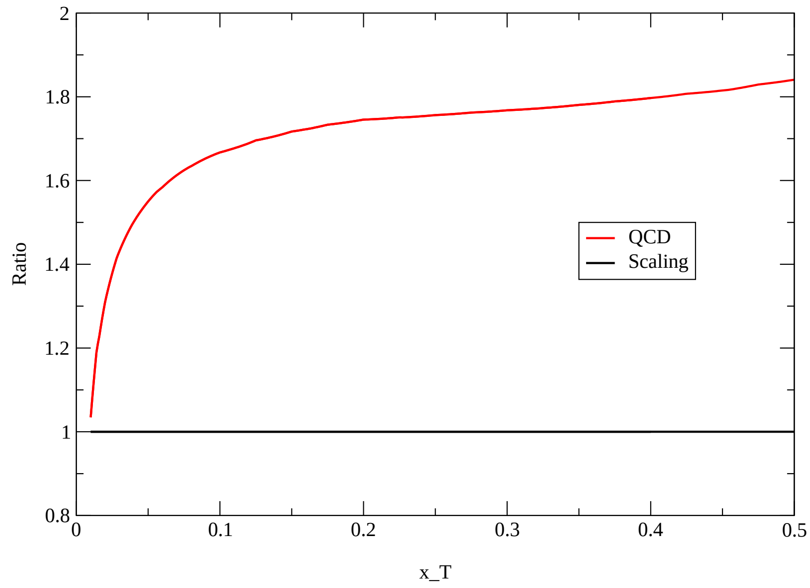


Figure 5: Ratio of $E_T^3 d^3\sigma/dE_T/d\eta_1/d\eta_2$ at $\eta_1 = \eta_2 = 0$ for $\sqrt{s} = 630$ GeV and $\sqrt{s} = 1800$ GeV versus $x_T = 2E_T/\sqrt{s}$.

Scaling violations due to $\mu_R = \mu_F = E_T$ from strong coupling and evolution of parton densities.

# Alternate variables

Can also work in terms of the dijet mass $M_{JJ}$ and the centre-of-mass scattering angle $\theta^*$

$$
\begin{aligned}
M_{JJ}^2 &= 4E_T^2 \cosh^2 \eta^*, \\
\cos\theta^* &= \tanh \eta^*, \\
t &= -\frac{s}{2}(1-\cos\theta^*)
\end{aligned}
$$

so that

$$
\begin{aligned}
\frac{d^3\sigma}{dM_{JJ}^2 d\cos\theta^*} &\sim \int dx_1 dx_2 F(x_1,\mu_F)\ F(x_2,\mu_F)\delta(x_1 x_2 s - M_{JJ}^2) \\
&\times \frac{\alpha_s^2(\mu_R)}{32\pi M_{JJ}^2} |\mathcal{M}_{gg\to gg}|^2
\end{aligned}
$$

where now at small $t$ (large $\cos\theta^*$)

$$
\begin{aligned}
|\mathcal{M}_{gg\to gg}|^2 &\sim \left(\frac{s}{t}\right)^2, \\
&\sim \frac{1}{(1-\cos\theta^*)^2},
\end{aligned}
$$

the classic Rutherford scattering behaviour for the exchange of a massless vector boson in the $t$-channel.

# Alternate variables

An even better variable is

$$\chi = e^{2\eta^*} = \left(\frac{1+\cos\theta^*}{1-\cos\theta^*}\right)$$

that removes the singular behaviour as $t \to 0$, $\cos\theta^* \to 1$

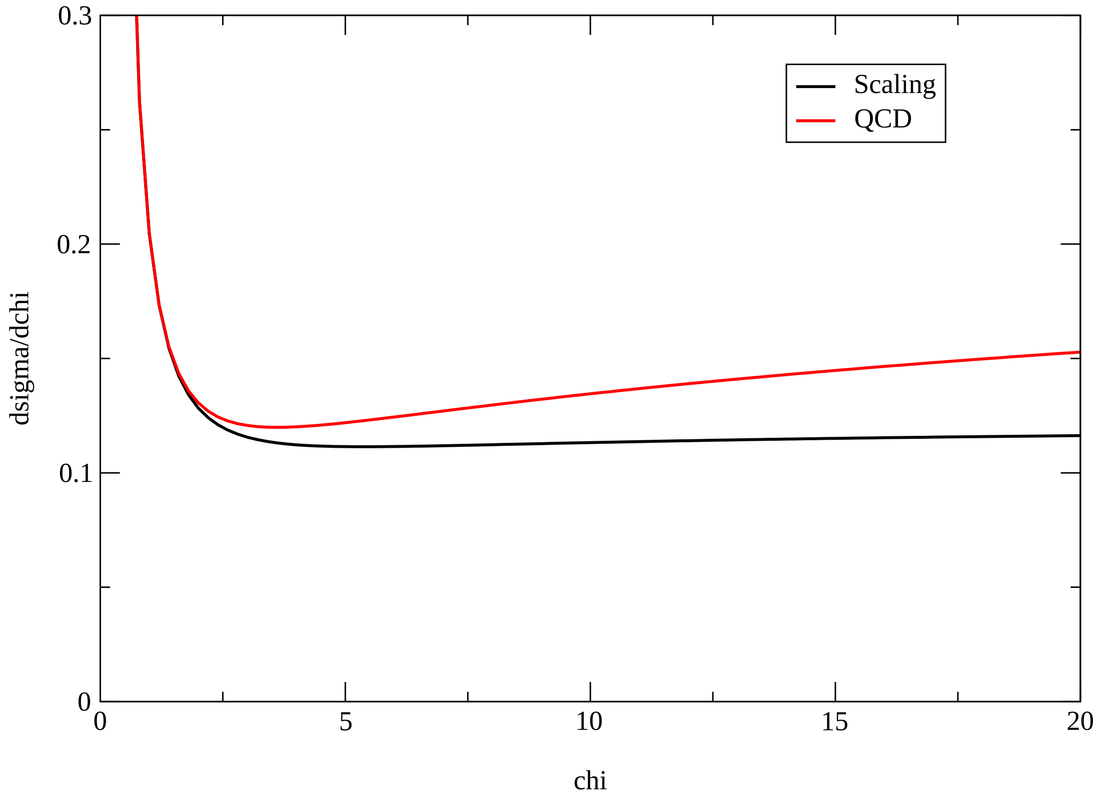


Figure 6: $d\sigma/d\chi$ for $M_{JJ} = 200$ GeV, $\eta^{\rm boost} = 0$ and $\sqrt{s} = 2$ TeV.

Scaling violations due to $\mu_R = \mu_F = E_T$ from strong coupling and evolution of parton densities.

# The unphysical scales - $\mu_R$

The renormalisation scale $\mu_R$ is introduced when redefining the bare fields in terms of the physical fields at scale $\mu_R$. It is unphysical - and the answer shouldnt depend on it - but does because we work at a fixed order in perturbation theory. Therefore, you can choose any value (within reason). Typical values are the hard scale in the process $\mu_R \sim E_T$.

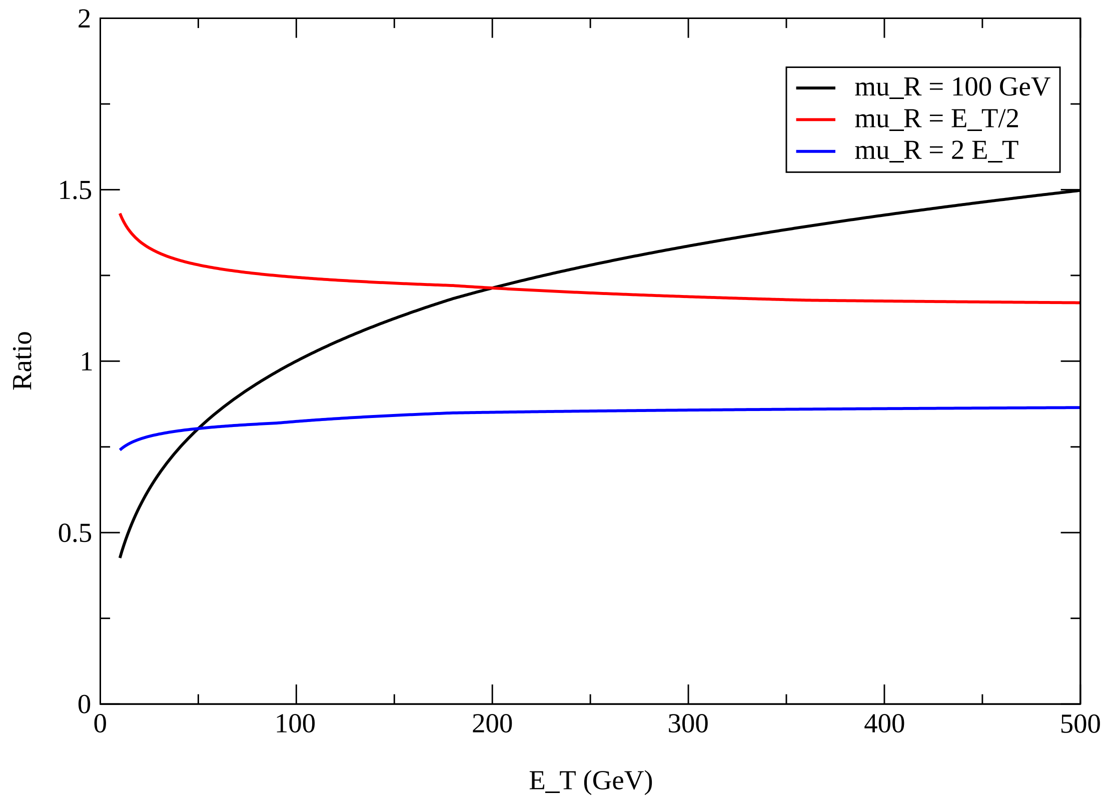


Figure 7: $\alpha_s^2$ for various values of $\mu_R$ compared to $\mu_R = E_T$.

# The unphysical scales - $\mu_F$

The factorisation scale $\mu_F$ is introduced when absorbing the divergence from collinear radiation into the parton densities. It is unphysical - and the answer shouldnt depend on it - but does because we work at a fixed order in perturbation theory. Typically, we think of radiation at a transverse scale $> \mu_F$ as being detectable so that $\mu_F \sim E_T$ is a reasonable choice.

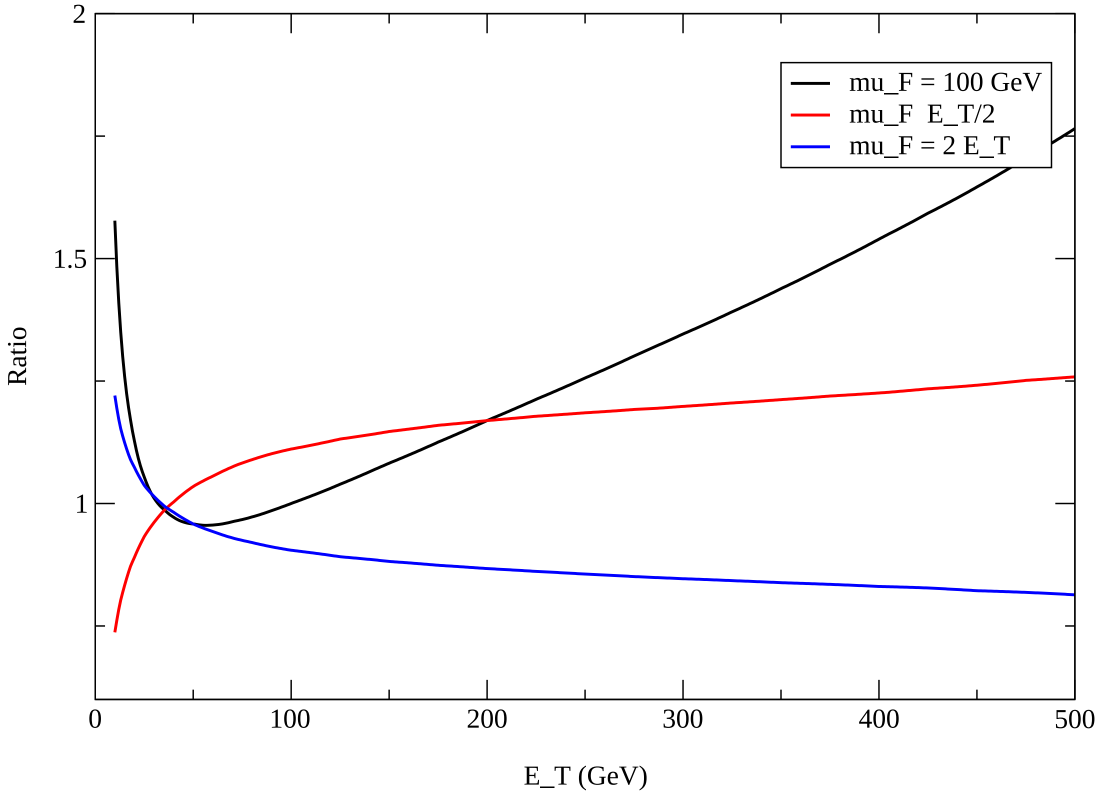


Figure 8: The parton-parton luminosities for various values of $\mu_F$ compared to $\mu_F = E_T$ at $\eta_1 = \eta_2 = 0$.

# Jet algorithms

So far, at leading order the jet is represented by a single parton.

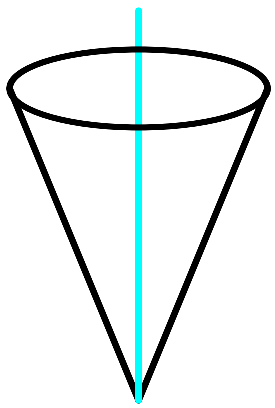

$\Longrightarrow$ it doesnt matter what the jet definition is... (unless we deal with multiparton configurations and we want to separate the partons)

$\Longrightarrow$ motivations for higher order corrections are to

- improve the matching between theoretical and experimental jets
- reduce the dependence on the unphysical scales (see later)
- identify kinematic regions where logarithms are large
- model radiation outside of the jet

# Structure of NNLO

Example, pure gluon ingredients to $pp \to 2$ jets

- 1 loop, 2 parton final state

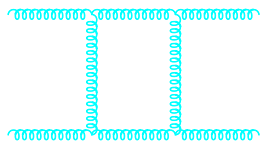

  Same kinematics as leading order - single parton $\equiv$ jet

- tree level, 3 parton final states
  or 2+1 parton final state

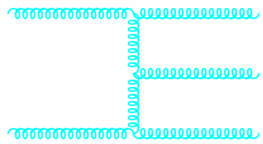

  Different kinematics - extended phase space and now have the possibility of partons combining to form jet

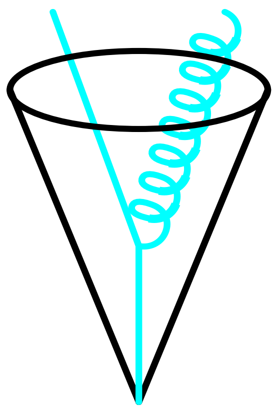

  $\Longrightarrow$ sensitivity to jet algorithm - size of jet and way in which momenta are combined

- Note both contributions are divergent and it is a technical issue to cancel the divergences and make finite physical predictions

# NLO phase space

- The parton fractions are given by

$$x_{1,2} = \frac{E_{T1}}{\sqrt{s}} \left( \exp(\pm\eta_1) + \frac{E_{T2}}{E_{T1}} \exp(\pm\eta_2) + \frac{E_{T3}}{E_{T1}} \exp(\pm\eta_3) \right),$$

  where $E_{T1} > E_{T2} \geq E_{T3}$.

- Since the transverse energies of the partons are no longer forced to be equal, $|\eta_2|$ may increase to compensate for having a smaller transverse energy, $E_{T2}/E_{T1} < 1$.

- The maximum possible values of $|\eta_2|$ occur when $E_{T2} = E_{T3}$,

$$-\log\left(\frac{a\bar{a} + \sqrt{a^2\bar{a}^2 - a\bar{a}}}{a}\right) < \eta_2 < \log\left(\frac{a\bar{a} + \sqrt{a^2\bar{a}^2 - a\bar{a}}}{\bar{a}}\right),$$

  where

$$\begin{aligned} a &= \frac{(2 - x_{T1}\exp(\eta_1))}{x_{T1}} \\ \bar{a} &= \frac{(2 - x_{T1}\exp(-\eta_1))}{x_{T1}} \end{aligned}$$

- The maximum allowed value of $|\eta_1|$ is unchanged at next-to-leading order

- Adding more partons into the final state further increases the allowed $\eta_2$ range corresponding to the production of more and more soft partons.

# NLO phase space cont'd

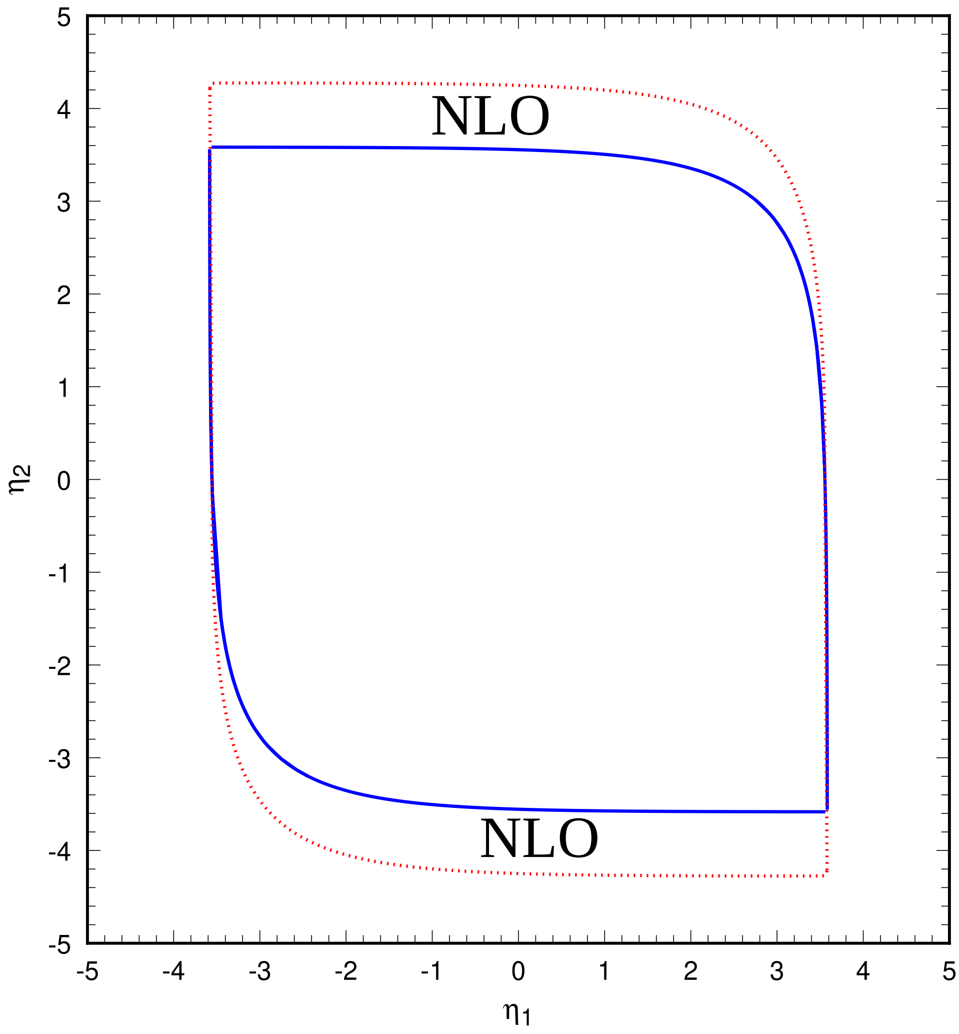


Figure 9: Phase space for $E_T = 50$ GeV and $\sqrt{s} = 1.8$ TeV.

- The physical cross section will exhibit a rather sharp cutoff as $|\eta_1|$ increases.
- There will be a more gradual fall off in the cross section as $|\eta_2|$ increases.

# NLO matrix elements

The matrix elements for

$$a(p_1) + b(p_2) \longrightarrow c(p_3) + d(p_4) + e(p_5)$$

averaged (summed) over initial (final) state colours and spins are

$$\begin{aligned} |\mathcal{M}_{qq'\to qq'g}|^2 &= \frac{4}{9} g^6 \left( \frac{s^2 + s'^2 + u^2 + u'^2}{tt'} \right) \\ \times & \quad (2C_F ([14] + [23]) \\ & \quad + \frac{1}{N} (2[12] + 2[34] - [13] - [14] - [23] - [24])) \end{aligned}$$

where (since $p_5 \neq 0$) the primed and unprimed variables are different

$$\begin{aligned} s &= (p_1 + p_2)^2, & t &= (p_1 - p_3)^2, & u &= (p_2 - p_3)^2 \\ s' &= (p_3 + p_4)^2, & t' &= (p_2 - p_4)^2, & u' &= (p_1 - p_4)^2 \end{aligned}$$

and the eikonal factor

$$[ij] = \frac{p_i.p_j}{p_i.p_5 \; p_5.p_j}$$

accounts for the coherent radiation of gluons from the quarks

Exercise: Draw down the five Feynman diagrams for $qq' \to qq'g$

# NLO matrix elements cont'd

In the limit that the gluon is either soft ($p_5 \to 0$) or collinear with one of the quarks, the matrix element factorises

$$|\mathcal{M}_{qq'\to qq'g}|^2 \to |\mathcal{M}_{qq'\to qq'}|^2 X$$

where $X$ is a factor that contains the infrared singular terms and

$$|\mathcal{M}_{qq'\to qq'}|^2 = \frac{4}{9} g^4 \left( \frac{u^2 + s^2}{t^2} \right)$$

For example, in the soft limit $s' \to s$, $t' \to t$ and $u' \to u$ so that by trivial inspection,

$$\begin{aligned} X \quad = \quad & 2g^2 \Bigg\{ 2C_F\left([14] + [23]\right) \\ & \quad + \frac{1}{N}\left(2[12] + 2[34] - [13] - [14] - [23] - [24]\right) \Bigg\} \end{aligned}$$

with

$$[ij] = \frac{p_i.p_j}{p_i.p_5 \; p_5.p_j}$$

diverging in the $p_5 \to 0$ limit.

Soft factors like this dictate all interjet coherence phenomena

# Exercise

In the limit where $p_4$ and $p_5$ are collinear (so $p_4.p_5 \to 0$), make the replacements

$$p_4 = (1-z)p_{45}, \qquad p_5 = \; p_{45}$$

so that

$$s' = 2p_3.p_4 \to (1-z)2p_3.p_{45} = (1-z)s$$

etc and

$$[i4] = \frac{p_i.p_4}{p_i.p_5 \; p_4.p_5} \to \frac{(1-z)p_i.p_{45}}{zp_i.p_{45} \; p_4.p_5} = \frac{1-z}{z} \, \frac{1}{p_4.p_5}.$$

Hence show that

$$|\mathcal{M}_{qq' \to qq'g}|^2 \to |\mathcal{M}_{qq' \to qq'}|^2 X$$

where (ignoring terms that do not diverge in the collinear limit)

$$X = C_F g^2 \, \frac{4}{p_4.p_5} \, \frac{1+(1-z)^2}{z}$$

— the splitting function for a quark to radiate a collinear gluon.

# Overall effect of NLO corrections

$$R = \frac{d^3\sigma^{NLO}/dE_T d\eta_1 d\eta_2}{d^3\sigma^{LO}/dE_T d\eta_1 d\eta_2}$$

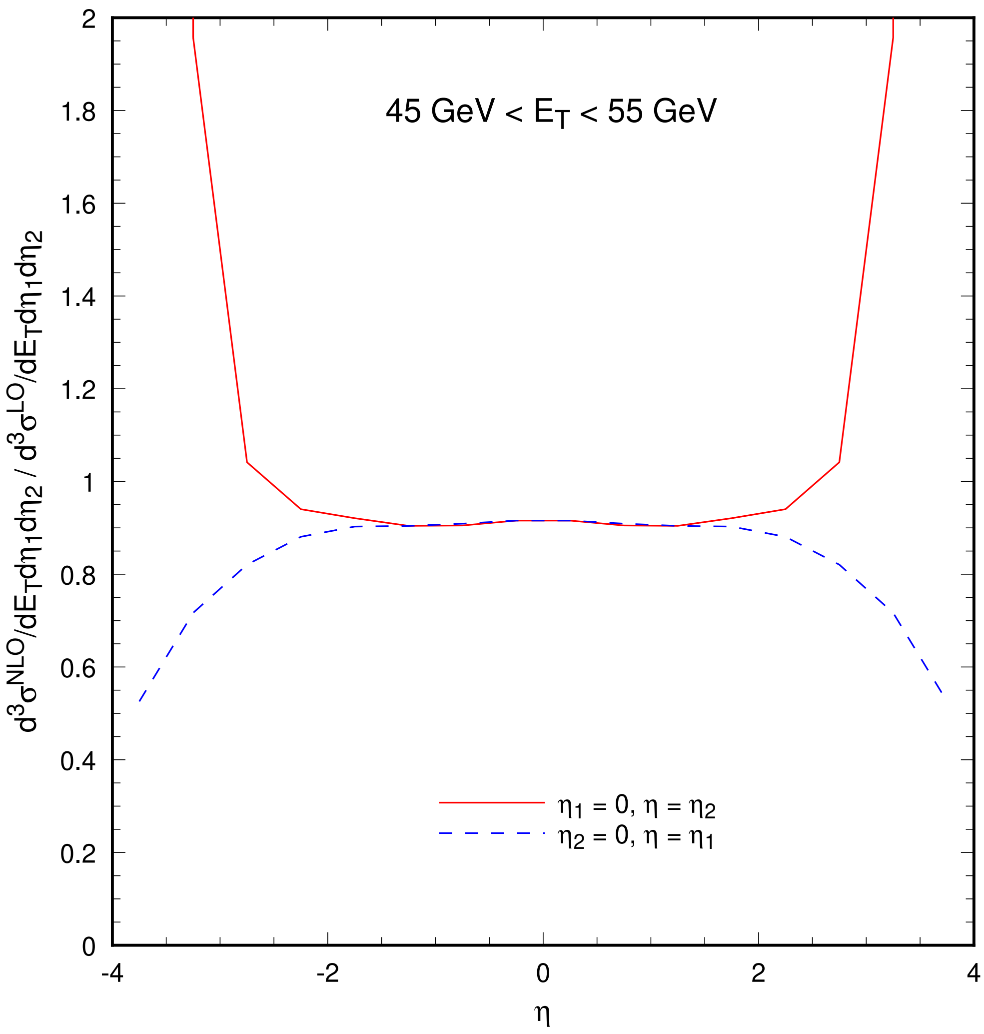


Figure 10: $K$-factor for $E_T = 45 - 55$ GeV and $\sqrt{s} = 1.8$ TeV.

Moderate corrections away from phase space boundaries - identify large logarithmic corrections at large $\eta_2 \Longrightarrow$ re-summation.

# Renormalisation scale dependence

$$\frac{d\sigma}{dE_T} = \alpha_s(\mu_R)^2 A + \alpha_s(\mu_R)^3 (B + 2b_0 L A) + \alpha_s(\mu_R)^4 \left(C + 3b_0 L B + (3b_0^2 L^2 + 2b_1 L) A\right)$$

with $L = \log(\mu_R/E_T)$ and $b_i$ the known beta function coefficients.

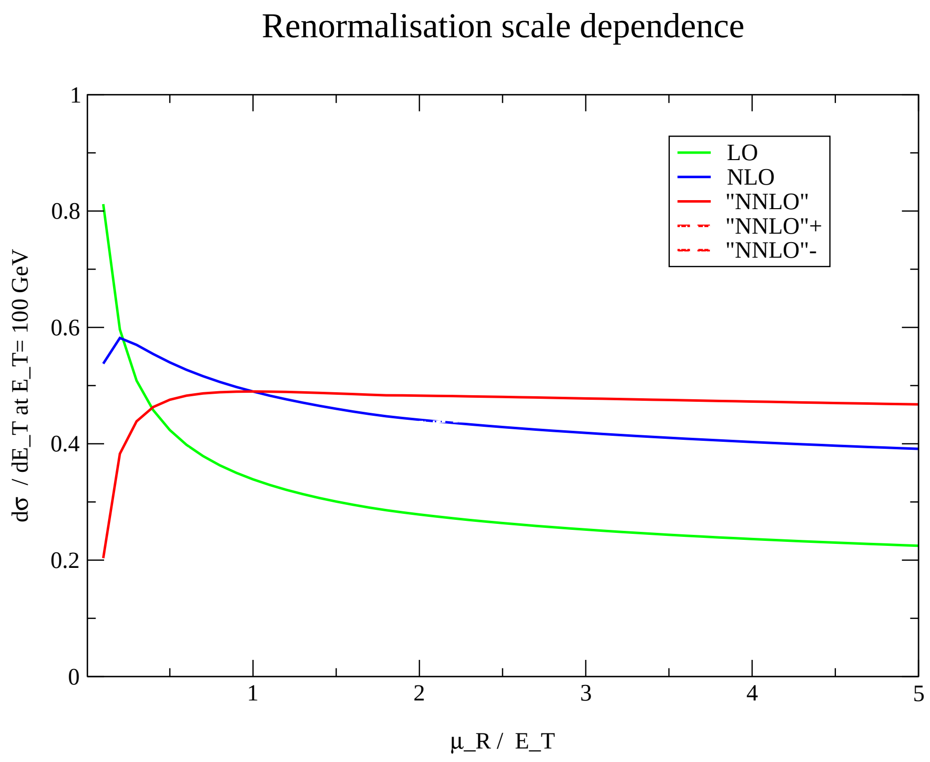


Figure 11: Single jet inclusive distribution at $E_T = 100$ GeV and $0.1 < |\eta| < 0.7$ at $\sqrt{s} = 1800$

The NNLO coefficient C is unknown. The curves show the guesses $C = 0$ (solid) and $C = \pm B^2/A$ (dashed).

# Jet algorithm

Must be infrared safe:

- Infrared problem - adding an infinitely soft parton should not change the number of jets

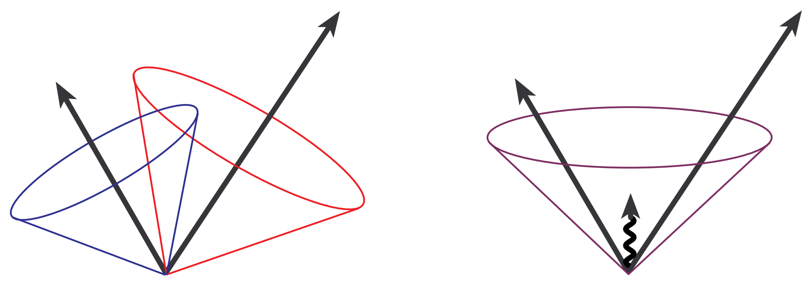

- Collinear problem - replacing any massless parton with an exactly collinear pair of massless partons should not change the number of jets

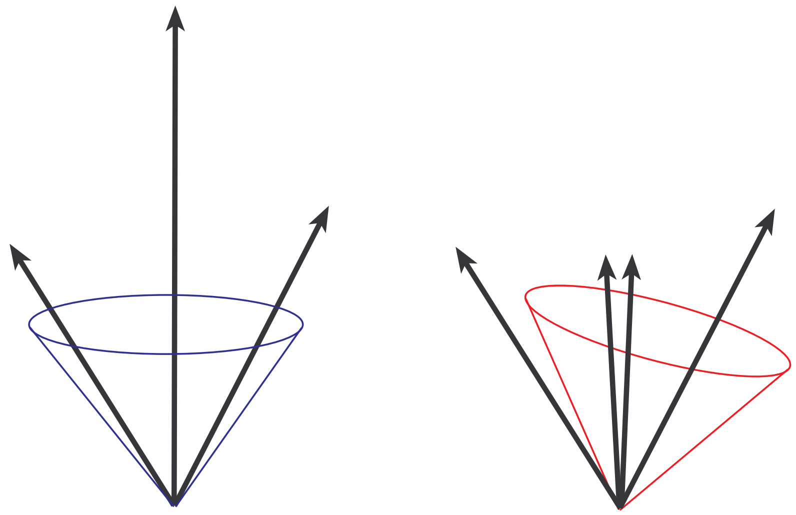

+ insensitive to hadronisation
+ insensitive to longitudinal boosts

# Jet definitions

The transverse energy, $E_T$, pseudorapidity, $\eta$, and azimuth, $\phi$, of a jet are given by:

$$\begin{aligned} E_{T\mathrm{jet}} &= \sum_{i \in \mathrm{jet}} E_{Ti}, \\ \eta_{\mathrm{jet}} &= \sum_{i \in \mathrm{jet}} E_{Ti}\, \eta_i / E_{T\mathrm{jet}}, \\ \phi_{\mathrm{jet}} &= \sum_{i \in \mathrm{jet}} E_{Ti}\, \phi_i / E_{T\mathrm{jet}}. \end{aligned}$$

We shall always use boost-invariant variables, so 'angle'means the Lorentz-invariant opening angle

$$R_{ij} = \sqrt{(\eta_i - \eta_j)^2 + (\phi_i - \phi_j)^2}$$

# $k_T$ algorithm

- For every pair of particles, define a closeness

$$d_{ij} = \min(E_{Ti}, E_{Tj})^2 R_{ij}^2 \left(\approx \min(E_i, E_j)^2 \theta_{ij}^2 \approx k_\perp^2\right).$$

- For every particle, define a closeness to the beam particles,

$$d_{ib} = E_{Ti}^2 R^2.$$

- If $\min\{d_{ij}\} < \min\{d_{ib}\}$, merge particles $i$ and $j$
- If $\min\{d_{ib}\} < \min\{d_{ij}\}$, jet $i$ is complete.

These steps are iterated until all jets are complete. In this case, all opening angles within each jet are $< R$ and all opening angles between jets are $> R$.

Note: not every particle within $R$ of the jet axis is included - the cone has a flexible edge.

# The cone algorithm

- For every seed tower sum all cells within angle $R$
- Recompute jet direction and iterate until stable jet direction found
- If jets overlap, merge and split jet

Note that despite the use of a fixed cone of radius $R$, jets can contain energy at angles greater than $R$ from their direction, because of merging procedure.

- At the NLO parton level, additionally require that the two partons must be within $R_{\rm sep} R$ of each other — this is ad hoc parameter not present in experimental algorithm.
- New midpoint or improved legacy cone algorithm where pseudo-seed towers placed midway between jets with $R < \Delta R < 2R$ corresponds to $R_{\rm sep} = 2$.
- $k_T$-algorithm corresponds to $R_{\rm sep} = 1$.

# Jet shape

The jet shape can be defined as

$$\Psi(r;R) = \frac{\sum_i E_{Ti}\Theta(r - R_{ijet})}{\sum_i E_{Ti}\Theta(R - R_{ijet})}$$

where the sum is over the particles in the jet.

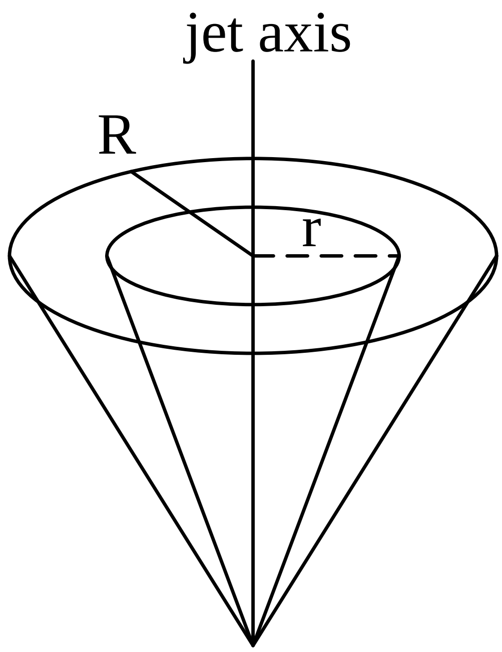


$\Psi$ is the fraction of energy of a jet of size $R$ contained in a sub-cone of size $r$ so that

$$\Psi(R;R) = 1$$

Here work with differential jet shape weighted by $r$

$$r\psi(r,R) = r\frac{d\Psi(r,R)}{dr}$$

# Jet shape cont'd

There are two (perturbative) contributions

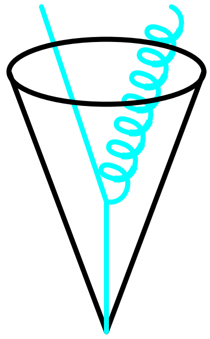

- Radiation inside the jet
  modelled by collinear splitting

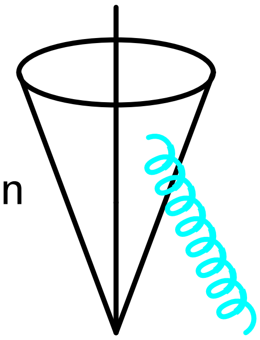

- Soft gluons falling into the cone
  modelled by coherent soft radiation pattern

# Radiation in jet

The probability of final-state emission from a parton of type $a$

$$dP_a = \frac{1}{2} \sum_b \frac{\alpha_s}{2\pi} \frac{d\rho^2}{\rho^2} \, dz \, P_{a\to bc}(z),$$

where $z$ is the fraction of $a$'s energy carried by $b$, and $\rho$ is the opening angle between the partons.

The phase space limits come from the requirements that both partons be within $R$ of the jet axis, and the opening angle be less than $R_{\text{sep}}R$.

Doing the integration over $z$, we find for quark and gluon jets

Seymour hep-ph/9707338,

$$\begin{aligned} r\psi_q(r) &= \frac{C_F\alpha_s}{2\pi}\left[2\left(-2\log Z - \frac{3}{2}(1-Z)^2\right)\right], \\ r\psi_g(r) &= \frac{C_A\alpha_s}{2\pi}\left[2\left(-2\log Z - (1-Z)^2\left(\frac{11}{6} - \frac{1}{3}Z + \frac{1}{2}Z^2\right)\right)\right] \\ &+ \frac{T_R N_f \alpha_s}{2\pi}\left[2(1-Z)^2\left(\frac{2}{3} - \frac{2}{3}Z + Z^2\right)\right], \end{aligned}$$

where

$$Z = \begin{cases} \frac{r}{r+R} & \text{if } r < (R_{\text{sep}}-1)R, \\ \frac{r}{R_{\text{sep}}R} & \text{if } r > (R_{\text{sep}}-1)R \end{cases}.$$

# Soft radiation from outside the jet

This is due to soft initial-state radiation that happens to be inside the jet cone by chance,

$$dP = 4\frac{C\alpha_s}{2\pi}\,d\eta\,\frac{d\omega}{\omega} \sim 4\frac{C\alpha_s}{2\pi}\,\rho d\rho\,\frac{dz}{z}$$

with colour factor $C \sim C_F \sim C_A/2$.

Applying the phase space limits gives

$$r\psi_i(r) = \frac{C\alpha_s}{2\pi}\left[2r\left(\frac{1}{Z^2} - 1\right)\right].$$

Initial radiation is insensitive to the jet direction, but this still gives a finite contribution as $r \to 0$. This is due to the fact that soft partons anywhere in the jet will pull the jet axis away from the hard parton direction.

Note: we are making small angle approximations so these simple formulae will make an error at large values of $R$ and $R_{\text{sep}}$.

# Soft radiation from outside the jet

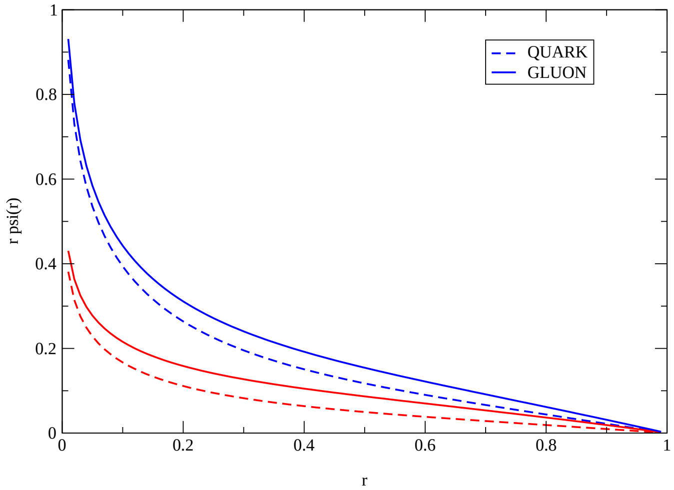


Figure 12: $r\psi(r;R)$ for quark and gluon jets with $E_T = 100$ GeV using the $K_T$ algorithm — $R = 1$, $R_{\rm sep} = 1$. The dashed line shows the effect of neglecting the out-of-cone contribution.

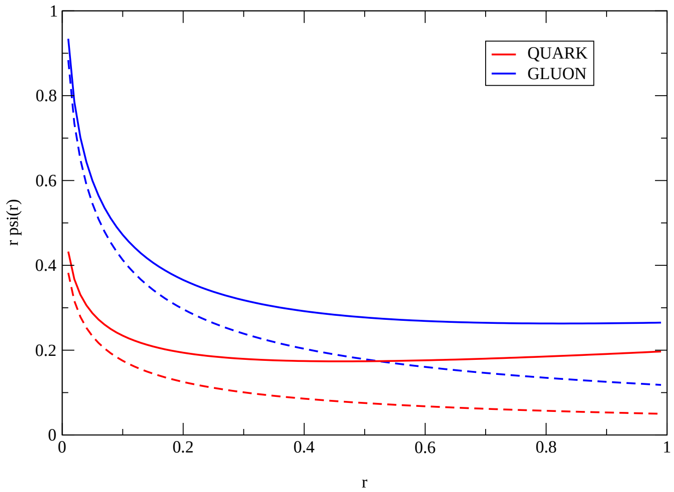


Figure 13: $r\psi(r;R)$ for quark and gluon jets with $E_T = 100$ GeV using the cone algorithm — $R = 1$, $R_{\rm sep} = 2$

$\Longrightarrow$ $k_T$ algorithm clearly better

# Other effects

- power corrections
  can be estimated using a running coupling $\alpha_s \longrightarrow \alpha_s(zrE_T)$
  $\Longrightarrow$ significant changes to model prediction - shifts shape to right
- infrared logarithms
  As $r \longrightarrow 0$, the energy profile develops large logs $\sim \alpha_s^n \log^{2n-1} r$
  $\Longrightarrow$ can be resummed using standard techniques

Seymour hep-ph/9707338,

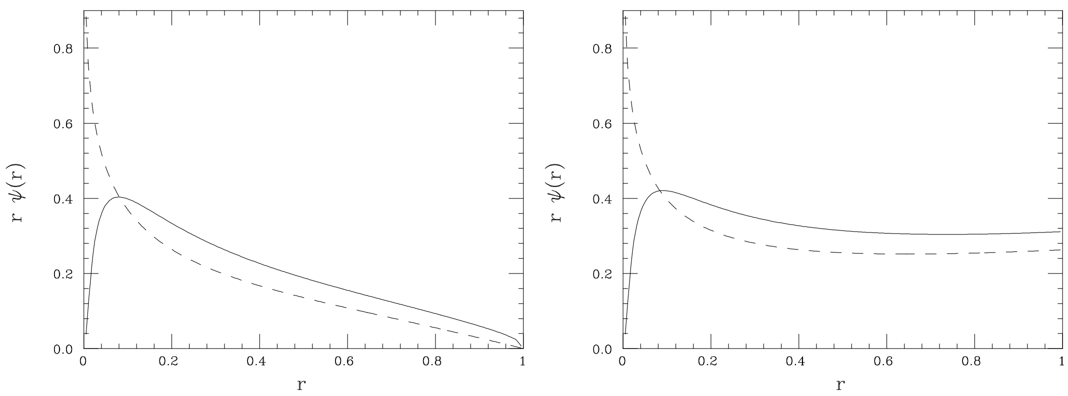


Figure 14: $r\psi(r;R)$ for jets with $E_T = 100$ GeV using the $K_T$ algorithm ($R = 1$, $R_{\rm sep} = 1$) and the cone algorithm ($R = 1$, $R_{\rm sep} = 2$). The solid line is the resummed result including power corrections.

# What to expect at the LHC!

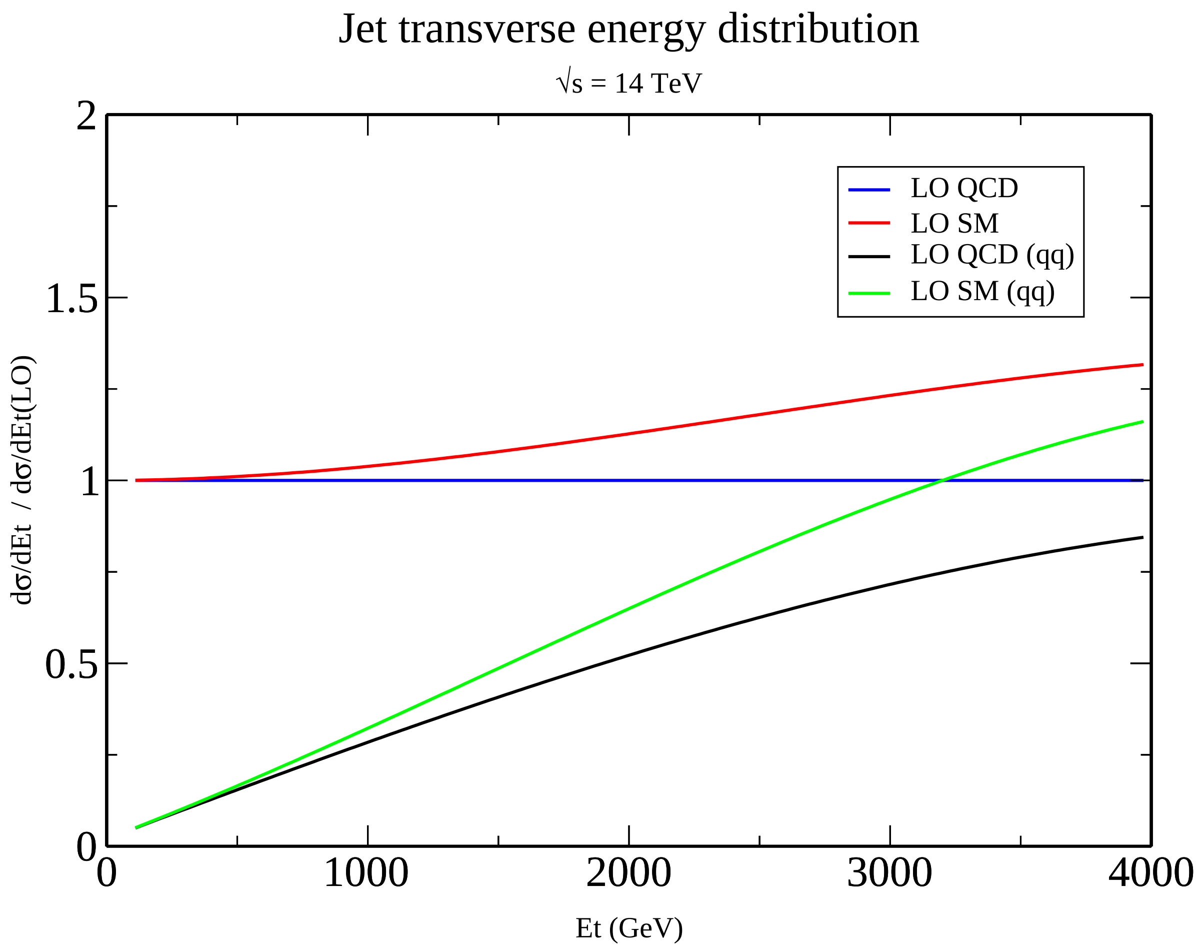


Will see same sort of rise over QCD as jet energy increases.

Due to new physics? or old physics?

In fact it is Standard Model $\mathcal{O}(\alpha_s \alpha_w)$ contributions to $qq$ scattering processes - interference of $t$-channel $Z$ exchange with $u$-channel gluon exchange.

# ... and now

Seen how jets look in theory - now for what they really look like $\Longrightarrow$ Nikos Varelas